since 1961

Baltica

BALTICA Volume 39 Number 1 June 2026: 58–72
https://doi.org/10.5200/baltica.2026.1.6

Research article

Mizarai impact structure in Lithuania: structural, petrological, and geochemical characteristics

Gediminas Motuza*, Dainius Michelevičius, Agnė Druskytė, Rokas Zamžickas, Jonas Liugas

Motuza, G., Michelevičius, D., Druskytė, A., Zamžickas, R., Liugas, J. 2025. Mizarai impact structure in Lithuania: structural, petrological, geochemical characteristics. *Baltica 38 (2)*, 58–72. Vilnius. ISSN 1648-858X.
Manuscript submitted 24 June 2024 / Accepted 28 March 2026 / Available online 04 May 2026

Abstract. The paper provides an overview of the Mizarai impact structure located in southern Lithuania, discovered in the course of geological mapping in 1969 and identified in 1975. Since then, the structure has been investigated by the mapping of gravity and magnetic fields, 2D and 3D seismic surveys, drilling and core studies. The structure is in the form of an oval depression situated within the Precambrian crystalline basement filled with presumably Ediacaran to Lower Cambrian detrital sediments derived from target rocks and ejecta and overlined with Mesozoic and Quaternary sediments. Gravity and seismic data have not indicated the presence of a central uplift within the Mizarai depression, suggesting a simple form. We estimate that the recent size of the crater is 3.8 × 4.2 km, after erosion in the course of ~ 300 Ma. Before erosion, the primary crater had a rim-to-rim diameter of up to 5 km and a depth of approximately 1 km. The impact metamorphism manifested in the transformation of target rocks into impact breccias and impact melt rocks, displaying shock features such as shatter cones, isotropization of quartz and plagioclase, planar deformation features (PDFs) in quartz, and kink-bands in biotite. While most impactites reflect the target rock composition, suevitic impact breccias and impact melt rocks (glass) are enriched by potassium.

Keywords: *simple hypervelocity impact crater; impact rocks; shock metamorphism; 3D seismic exploration; crystalline basement*

✉ *Gediminas Motuza* (gediminas.motuza@gf.vu.lt) https://orcid.org/ 0000-0002-5943-6306,*
Vilnius University, Vilnius, Lithuania;
Dainius Michelevičius (dmi@geobaltic.lt),
GeoBaltic JSV;
Agnė Druskytė,
Rokas Zamžickas (rokaszamzickas@gmail.com)
Vilnius University, Vilnius, Lithuania;
Jonas Liugas (jonas.liugas@gamtc.lt),
Nature Research Centre, Vilnius, Lithuania

**Corresponding author*

INTRODUCTION

The Mizarai hypervelocity impact structure (astrobleme) is located in southern Lithuania, in the vicinity of the Druskininkai resort (Fig. 1). The structure is in the form of an oval depression (crater) in the Precambrian crystalline basement, filled by presumably Lower Cambrian to Ediacaran sediments, overlined with Triassic, Cretaceous and Quaternary deposits of a total thickness of up to 372.5 m. It is partly eroded, its present rim-to-rim size on the surface of the Precambrian crystalline basement is around 3.8 × 4.2 km. (Fig. 1). In the recent international stratigraphic chart, the Lower Cambrian as a stratigraphic unit does not exist. We use it in the sense of referred publications.

The time of impact presumably corresponds to the age of crater-fill sediments. Since the discovery of the structure, several studies were carried out, some quite recently; however, only a few short papers and con-

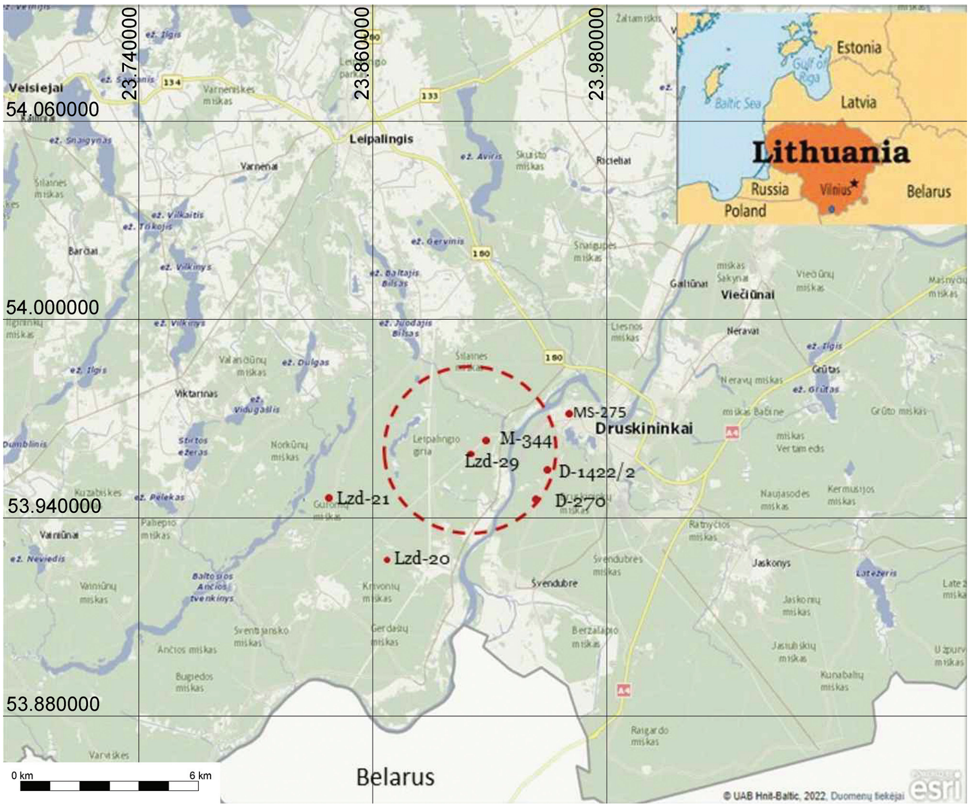

Fig. 1 Geographic position of the Mizarai hypervelocity impact crater – red circle and blue dot in the insert. Red points – boreholes

ference abstracts were published, just superficially characterizing the crater and its origin.

The purpose of this article is to characterize the structure, morphology, petrology and geochemistry of the Mizarai impact crater, summarizing available geophysical data, results of examination of thin sections and geochemical analyses of target and impact rocks.

THE HISTORY AND METHODS OF RESEARCH

The general characteristic of the structure of Mizarai depression, its surrounding and regional context is based on the geological mapping of the crystalline basement carried out in southern Lithuania, involving a preliminary mapping of the gravity and magnetic fields.

The first information on the Mizarai object appeared in 1969 when a local negative gravity anomaly in the form of a nearly regular ring was mapped by R. Apirubytė and N. Gedvilaitė (Apirubytė, Gedvilaitė 1969). To check this anomaly, the borehole Druskininkai-270 was drilled in its marginal part, and a depression in the Precambrian crystalline basement, filled up with the sequence of interbedded sandstone, silt and conglomerate, containing fragments of glassy material, was discovered. This sequence was regarded as volcanic, and the depression was interpreted as a graben (Šliaupa, Stirpeika 1973).

A more detailed and precise mapping of gravity and magnetic fields was performed as part of the following geological mapping campaigns (Merkinė and Lazdijai projects). In the course of these projects, boreholes Merkinė-344 and Lazdijai-29 were drilled in the depression, and a few boreholes in its vicinity. The manuscript reports for these researches are stored in the Archives of the Lithuanian Geological Survey. The main authors of these reports are S. Marfin, G. Motuza, T. Skripkina, A. Šliaupa, and A. Žvykas. The borehole D-1422/2 was drilled in the crater for the exploration of mineral water (Table 1). The drill cores of all boreholes mentioned above are available on the core storage at the Lithuanian Geological Survey.

The first attempt of modelling based on gravimetric data, applying GM-SYS software was performed by L. Korabliova (Korabliova *et al.* 2003).

In 2018, geophysical company GeoBaltic implemented a project initiated by the Agency for Science, Innovation and Technology (MITA). The project aimed to develop and test a new seismodynamic field data acquisition method and IT management system to increase the efficiency of seismic field data acquisition.

During the project, three 2D seismic profiles with a total length of 20 km and a 3D seismic area of 22 sq km were acquired, using an accelerated weight drop system as a source and Nodal Sercel seismic recorder for data registration. Two 2D lines crossed the entire crater, while the 3D seismic survey covered the NW part of it (Fig. 4). Despite this, the acquired data essentially changed the former understanding of the size and structure of the crater.

In the course of the mapping, the obligatory drill core acquisition was followed by a petrological examination of rocks in thin sections under a polarizing microscope performed by R. Gailius, G. Motuza, T. Skripkina, and L. Chrianina. PDFs in quartz grains in the granite from borehole M-344 were studied by R. Gailius (Motuza, Gailius 1980), applying the conventional U-stage analysis (Dobrokhotova 1957).

The chemical composition of rocks was characterized by analyses for major oxides, produced by the

Table 1 The boreholes drilled in the Mizarai crater and its vicinity

Borehole and its abbreviation	Latitude	Longtitude	Elevation, AMSL, m	Bottom of the sedimentary cover, m	Bottom of the sedimentary crater fill, m	Total depth, m
Druskininkai-270 (D-270)	54.00369	23.94812	97.37	332.2	381.1	381.3
Druskininkai-1422/2 (D-1422)	54.00927	23.95188	95.7	327	367.8	385
Mizarai-344 (M-344)	54.01646	23.9195	114.5	372.5	525.7	610
Lazdijai-29 (Lzd-29)	54.0123	23.917	113	370.8	512.4	843
Meilės sala-275 (Ms-275)	54.02425	23.96145	92	292	-	302.4
Lazdijai-20 (Lzd-20)	53.9873	23.86756	110	321.5	-	391.2
Lazdijai-21 (Lzd-21)	54.00064	23.85007	110	325.8	-	366.4

Table 2 Average major element abundance in the fragments of the target rocks in the breccia from the Mizarai crater

Sample	Rock	SiO_2 %	Al_2O_3 %	Fe_2O_3 %	MgO %	CaO %	Na_2O %	K_2O %	TiO_2 %	MnO %
Lzd-29/515.6	Bt gneiss	56.15	18.14	6.55	6.1	2.46	4.6	1.26	0.71	0.09
Lzd-29/524.5	Gabbro	47.03	17.84	8.55	8.58	5.73	3.82	1.3	1.46	0.11
Lzd-29/526	Gabbro	48.13	17.84	9.41	8.58	3.64	4.6	0.95	1.57	0.13
Lzd-29/532	Bt gneiss	55.23	17.54	7.96	5.28	3.78	4.05	1.75	1.19	0.09
Lzd-29/534.8	Gabbro	46.16	16.35	12	9.3	3.04	3.4	1.71	2.17	0.11
Lzd-29/540.8	Suevite	60.63	14.86	5.73	6.1	0.75	2.66	5.05	0.59	0.10
Lzd-29/542.2	Amphibolite	46.8	16.94	11.85	7.7	6.35	3.7	1.67	2.7	0.14
Lzd-29/546.2	Suevite	58.19	15.16	6.64	7.07	0.65	2.5	5.05	0.78	0.10
Lzd-29/567.9	Suevite	60.23	15.16	5.79	5.86	0.60	2.27	5.9	0.54	0.10
Lzd-29/591	Amphibolite	48.33	18.13	8.75	8.17	4.73	3.82	1.15	1.3	0.09
Lzd-29/596.9	Amphibolite	49.99	16.05	9.95	2.44	2.30	3.13	1.71	1.23	0.11
Lzd-29/599	Bt gneiss	59.90	13.97	8.83	6.24	2.7	3.00	2.15	0.92	0.10
Lzd-29/607.6	Bt gneiss	60.83	14.12	6.61	6.79	1.36	3.32	2.1	0.61	0.09
Lzd-29/623	Amphibolite	50.07	16.05	9.58	9.72	2.33	2.70	1.83	1.08	0.10
Lzd-29/635.6	Gabbro	47.73	16.05	9.59	9.44	4.44	3.40	1.75	1.08	0.11
Lzd-29/639.7	Gabbro	49.7	17.69	10.4	6.60	6.02	3.13	1.50	1.73	0.10
Lzd-29/666.8	Granite	69.89	13.38	3.64	1.93	0.50	3.35	5.44	0.61	0.55
Lzd-29/680.8	Granite	66.68	13.97	4.73	2.43	0.92	3.65	5.05	0.87	0.33
Lzd-29/692.5	Amphibolite	51.41	15.16	21.01	5.70	2.46	3.70	2.2	2.44	0.16
Lzd-29/723.7	Amphibolite	49.60	17.84	9.33	4.65	4.28	4.87	2.50	1.95	0.11
Lzd-29/735.2	Amphibolite	40.04	14.86	10.67	12.18	7.2	3.25	1.1	0.84	0.14
Lzd-29/752.9	Granite	71.09	14.12	2.44	1.48	0.45	3.55	5.17	0.29	0.03
Lzd-29/755	Schist	45.33	15.1	12.31	10.12	2.56	1.00	3.50	1.45	0.17
Lzd-29/758.4	Granite	65.01	15.51	4.41	2.76	0.90	3.66	5.54	0.49	0.07
Lzd-29/765.5	Granite	75.36	12.80	1.32	0.73	0.30	3.06	6.18	0.03	0.13
Lzd-29/769.4	Granite	73.89	13.51	1.86	1.21	0.30	3.90	4.3	0.22	0.04
Lzd-29/828.1	Bt schist	39.69	10,21	10.96	11.66	7.50	0.46	4.00	4,12	0.17
Lzd-29/841	Bt schist	56.40	17.73	4.88	6.52	0.72	1.45	6.00	0.54	0.09
M344/532.3	Qtz diorite	52.30	16.56	9.97	8.64	3.11	2.90	0.98	1.16	0.07
M344/533	Qtz diorite	62.18	15.80	7.64	3.16	3.86	3.31	1.56	0.88	0.12
M344/562	Granite	74.64	13.44	2.4	0.64	1.04	2.94	4.08	0.20	0.04
M344/574.8	Gabbro	50.00	16.92	9.42	7.50	4.32	3.18	1.02	1.16	0.09
M344/610	Granodiorite	58.28	18.64	5.24	3.84	4.58	3.94	0.98	0.54	0.05

"wet chemistry" technique in a laboratory of the Integrated Geological Enterprise (Lower).

The abundance of both major and trace elements in impact glass was estimated employing the ICP-MS technique in the Acme Laboratories, Vancouver, Canada, and in the Laboratory of the Geological Survey of Norway (Table 3).

By the examination of drill cores indications, of the shock metamorphism of target rocks were revealed and presumption on cosmic origin of the structure was made (Gailius *et al*. 1975; Motuza, Gailius 1980; Masaitis *et al*. 1980; Masaitis 1999; Puura *et al*. 1994; Graniczny *et al*. 2011; Zamžickas 2012; Baliukevičius, Grigienė 2015; Motuza *et al*. 2016).

REGIONAL POSITION

The Mizarai crater is formed in the Precambrian crystalline basement and is filled with presumably Ediacaran or Lower Cambrian sediments and covered by Mesozoic and Quaternary deposits.

The Precambrian basement in the area around the crater is predominantly composed of the following lithological units (Motuza 2022 and references therein):

- Supracrustal felsic gneisses, originally sedimentary and volcanic rocks of intermediate and acid composition, and amphibolite, primary basalt. The rocks are metamorphosed in the conditions of amphibolite facies and migmatized. The age of supracrustals is regarded Orosirian;
- Gabbro, diorite, granodiorite, and tonalite association united in the Randamonys intrusive suite, which marks the orogenic period of formation of crust in the region at about 1.84–1.80 Ga;
- Cratonic intrusions of granite and granodiorite of Mazury–Veisiejai and Kabeliai suites, intruded at 1.48–1.53 Ga ago.

The Mizarai crater is situated in the contact zone of the migmatized supracrustals, Randamonys pluton, and the numerous minor granitic bodies of the Mazury–Veisiejai suite. The sedimentary cover of the basement is composed of sedimentary rocks from the Triassic, Cretaceous, and Quaternary systems, with a total thickness of up to 372.5 m (Table 1).

A few kilometres to the north, there appear layers of Cambrian, Ordovician, Silurian, and Permian systems, but they are verging out before reaching the crater. This happens because southern Lithuania is part of the Mazury–Belarus anteclise, a few thousand square kilometres large platform area, where an uplift inhibiting the formation or preservation of sedimentary cover dominated in the course of the late Paleozoic and early Mesozoic.

The crater itself is filled up with clastic sediments – siltstone, sandstone, and conglomerate, in some intervals rhythmically layered. In the lower part of the section, there appear the fragments of crystalline and glassy rocks. The counterparts of this sequence are not known beyond the limits of the crater. The type and distribution of the crater-fill deposits indicate their formation in a small continental basin (lake) (Motuza *et al*. 2016).

In the upper part of the section of these sediments (int. 388.85–440.4 m in the drill core of the borehole M-344), the microfossils identified by L. Paškevičienė as acritarchs *Leiosphaeridia* sp. sp., *Leiosphaeridia crassa* sp., and algae, *Oscillatorites* sp., *Oscillatorites wernadskii,* correspondingly (Motuza, Gailius 1980), have been found.

In the crater-fill sediments of the boreholes M-344 and Lzd-29, the films of amorphous carbon material located on the surfaces of the siltstone layers have been noticed. In places, a complicated microstructure similar to late Precambrian algae was revealed using Raman spectroscopy (Motuza *et al*. 2016).

The stratigraphic connotation of these fossils is very approximate. They appear in the layers from the Late Neoproterozoic to Early Paleozoic but mainly are related to the Neoproterozoic. Therefore, the Ediacaran-Early Cambrian is regarded as the most plausible time of impact (Jankauskas 1989).

Directly on the basement and on the top of crater-fill sediments, the Triassic sedimentary sequence is lying. In the crater, the Triassic is a few tens of meters thicker and its foot is deeper than outside the crater. This might be explained by the compaction of the crater fill under the pressure of overlying rocks. This also means that the Triassic was the first system which formed the permanent cover of the crater after its formation. Thus, since Ediacaran or Early Cambrian, up to the Triassic, i.e. ~ 300 Ma, the Mizarai structure was exposed to erosion.

A few systems of faults have been revealed in the basement of southern Lithuania. Some faults cut the sedimentary cover. The most evident and oldest are the faults striking in the NE–SW direction. Along these faults, the mylonitization of various grades took place. Presumably, they were formed in the course of orogeny in the Orosirian period. The EW and NS trending faults have been formed in the Mesoproterozoic. Along these faults, brittle deformations are observed. The faults striking to the NW are revealed by some researchers, presuming their formation in the late Paleozoic (Suveizdis 2003; Čyžienė *et al*. 2007; Motuza *et al*. 2015; Motuza 2022). A more detailed analysis of the fault system in the Druskininkai area, including the Mizarai structure, was carried out in the course of mapping, based on structural data and paleogeographic reconstructions. Predominantly faults of NW–SE and NE–SW direction were revealed and interpreted as faults flanking graben (Baltrūnas, Šliaupa 1974).

STRUCTURAL PATTERNS

Initial structural interpretation of the crater

The boreholes contributing to the characteristic of the size and shape of the Mizarai crater are distributed irregularly. Four boreholes are drilled inside the crater (Table 1). Two of them are in the very centre of the structure, and two others adjacent to its eastern marginal part (Fig. 2). A few boreholes were drilled outside the crater, in the vicinity, but mainly along its eastern margin. In the gravity anomaly map, the Mizarai crater is manifested by a nearly regular circle shape negative gravity anomaly of approximately 3–4 mGal and a sharp gradient zone surrounding it from the eastern side. The best fit of borehole and gravity data at that time suggested interpretation of Mizarai crater as an almost regular 6 km diameter circle shape depression (Korabliova *et al*. 2003) (Fig. 2).

The boreholes M-344 and Lzd-29 have been drilled in the central part of the gravity anomaly, and both of them showed the highest thickness of the crater fill (141.6 and 153.2 m, correspondingly) (Figs 3, 4). The boreholes D-270 and D-1422 are located in the

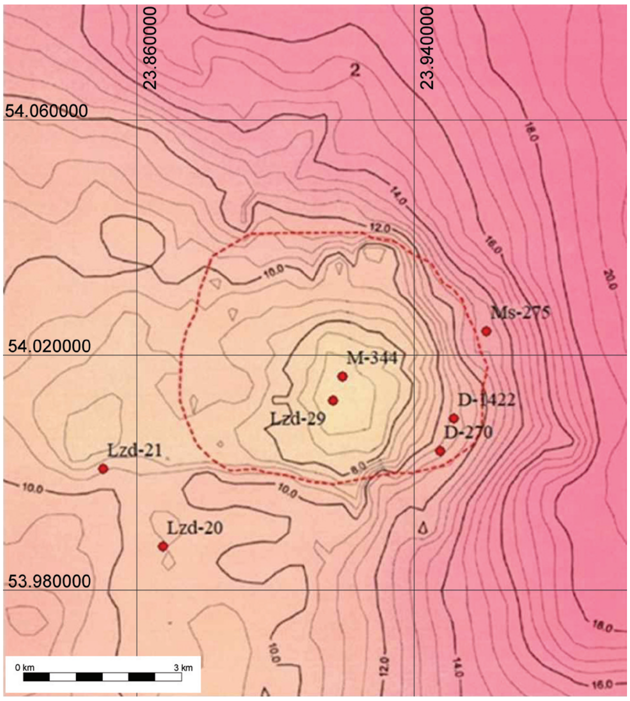

Fig. 2 Bouguer gravity anomaly map of the Mizarai crater (Korabliova *et al*. 2003). Isolines of the gravity field in milligals; red dotted line – earliest interpretation of crater shape based on borehole and gravity data

gravity gradient zone and appear inside the crater very close to its margin, indicating a relatively small thickness of 60–80 meters of the crater fill deposits. The borehole Ms-275 is located on the extension of the same gradient zone but appears outside the depression. Thus, the position of the eastern edge of the depression is marked by this narrow gradient zone. The position of its western limit is not reflected by the gravity field, because there the felsic rocks of low and little varying density are predominant (Fig. 2).

Structural interpretation based on recent seismic data

Initially, two seismic 2D lines were acquired, both crossing the whole structure of the crater, followed by a 3D seismic survey for the mapping of the whole depression more precisely (Fig. 4). The southern quadrant of the structure was not covered by 3D due to a complicated relief of the Nemunas River valley, dwelling area and its infrastructure. Despite this, the acquired data essentially changed the former understanding of the size and structure of the crater.

During seismic data interpretation, a few seismic reflectors were recognized in the sedimentary cover and on its contact with Precambrian basement (Fig. 3). Evident reflectors appear on the top of the sequence of crater-fill sediments and on its lower contact with the impact breccia of the rocks of Precambrian basement. The nature of these reflectors was confirmed by all boreholes drilled inside the crater (Table 1). Deeper reflectors have not been revealed by seismic surveys. The reflectors below the sedimentary crater fill are absent, which suggests a gradual transition from allochthonous to parautochthonous breccias.

The structural map of the top Precambrian seismic horizon prepared based on 3D seismic data (Fig. 4) indicates an almost circular, slightly flattened depression limited by a high gradient ring. This gradient zone is in places broadened out, which might reflect the local structural elements of tectonic origin, complicating the primary shape of the depression. At its centre, this model agrees with drilling data. The present minimal and maximal rim-to-rim size of the crater estimated this way is 3.8 × 4.2 km, which gives crater area more than twice smaller than it was in previous interpretation.

Crater size changes due to potential influence of erosion

Apparently, it is the pre-erosion diameter of the original ground surface (Osinski *et al*. 2022) that might be evaluated, taking into account its erosion, which varies in areas of diverse geological conditions and particular periods of geological history. The eval-

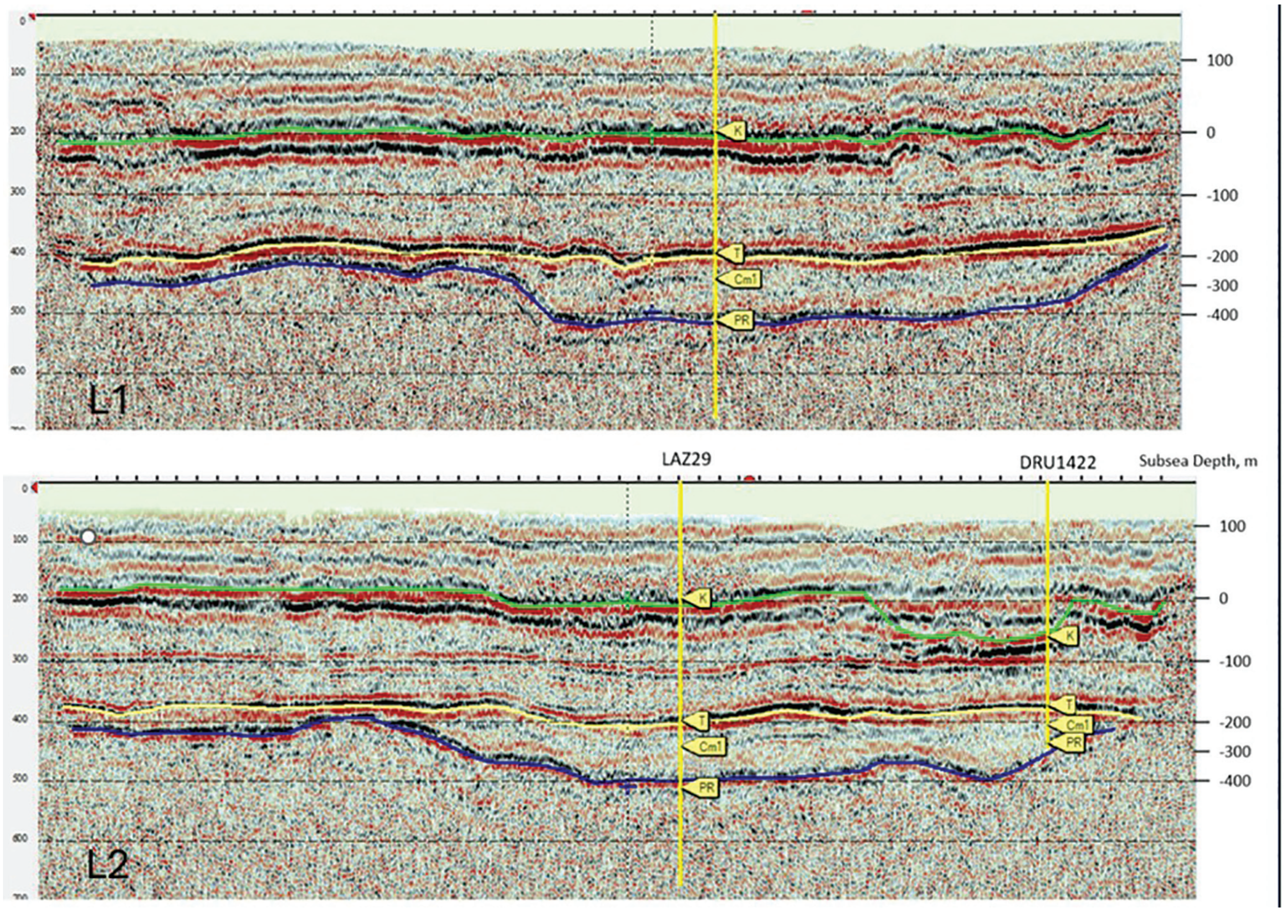

Fig. 3 Interpreted seismic sections L1 and L2 across the Mizarai crater (locations of seismic lines are shown in Fig. 4). Interpreted seismic reflectors: green – top of the Upper Cretaceous chalk covered by Quaternary, yellow – top of the Triassic sediments covered by Lower Cretaceous glauconitic sand, blue – top of Precambrian basement; left vertical scale is in milliseconds, right vertical scale is in meters

uated rate of erosion of the USA territory varies from 3.8 up to 61 mm/Ka (Judson, Ritter 1964).

For the area of Manicouagan crater, located on the Canadian shield, this figure in different periods is estimated to be 0.45 and 2.8 mm/Ka (Rondot 1994).

Particularly remarkable is the evaluation of the rate of cratonic denudation of southern Finland, which is comparatively close to Lithuania, both in terms of geographic distance and geological structure and evolution. Using various proxies, including data on impact structures, it was evaluated as 2.5 mm/Ka for the last 1.5 Gy (Hall *et al*. 2021).

For the area of Mizarai crater, the rate of erosion is not estimated. However, there are some data which might be useful for that purpose. In borehole Varėna-982, located 45 km to the north-east from the Mizarai crater, two samples of hornblende from metamorphic rocks have been dated by the Ar-Ar method (Bogdanova *et al*. 2001). The samples were taken from the depths of 471 and 771 m. The age obtained is 1.62 and 1.47 Ga, respectively. These figures mean the time of closure of the Ar-Ar system in hornblende, which occurs at around 550^{o}C. Presuming that the main fac-

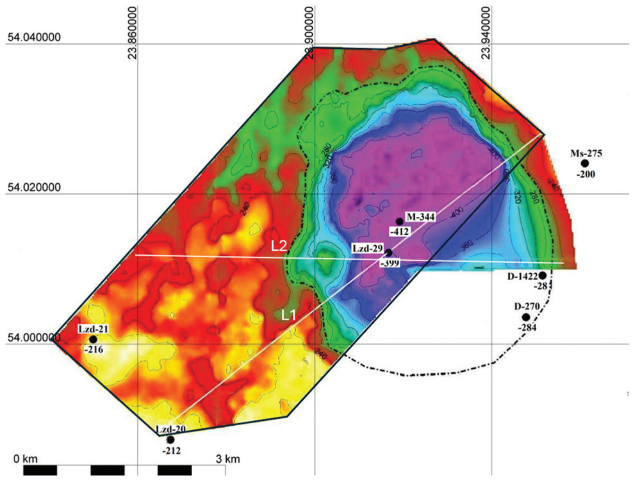

Fig. 4 The structural map of the top of the crystalline basement on the area of Mizarai crater. Isolines show top subsea depth of the crystalline basement, black dotted line – position of the recent edge of the crater, white line – position of the 2D seismic lines L1 and L2, black line – polygon of 3D seismic coverage

tor of cooling is the uplift and erosion, the 300-meter-thick sequence of the crystalline rocks was eroded in the course of 150 Ma, and the average rate of erosion was 2 mm/Ka. This figure fits well with the estimations of the rate of erosion in the area of the Manicouagan crater and in southern Finland presented above (Rondot 1994). The Mizarai crater was eroded in the course of 300 Ma at least since its formation presumably in Ediacaran or Early Cambrian up to Triassic, when it was finally covered by sediments. Assuming the same rate of erosion, for this time the erosion of the crust in southern Lithuania might reach 600 meters.

As a result of erosion, the diameter of the crater diminishes. For instance, the diameter of the Brent crater in Canada diminished by 225 m for 100 meters of erosion (Rondot 1994). Applying this rate to Mizarai, the erosion of 600 m diminished the diameter of the crater by 1.35 km. Thus, the apparent diameter of the crater on the original surface might be 5–5.5 km.

The depth of the crater taking the distance from the primary basement surface down to the surface of the autochthonous breccia is evaluated as 0.15–0.17 of apparent primary diameter (Koeberl 2002; Rondot 1994; Kenkmann 2021). Applying this ratio to the Mizarai structure, its primary depth might be up to 950 m. Presuming the erosion of 600 m and adding the thickness of sedimentary fill (150 m) and drilled section into allochthonous breccia (330 m), the depth of the crater might exceed 1000 m. These two estimations fit well, considering that the figures used in the calculation are very approximate and the contact between allochthonous and autochthonous breccia is transitional.

The terrestrial impact craters whose diameter exceeds 3–4 km obviously reveal the central peak (uplift) and terraced slope (French 1998). These features are regarded as indicative of the category of complex craters. However, newer data show that there are structures of Mizarai size or even larger in which central uplift is not observed. If the floor of such craters is flat but not bowl shaped, and they are distinguished as transitional craters. This is the case in Gow Lake, Canada, and Goat Paddock, Australia, both 5 km in diameter (Osinski *et al*. 2023). Based on recent data, the Mizarai crater should be classified as a simple ore transitional.

PETROLOGICAL CHARACTERISTIC OF IMPACTITES

Impactites are defined as a collective term for all rocks formed or affected by the impact (Koeberl 2002). The systematics and nomenclature of impactites applied here follow the recommendations of the IUGS (Stöffler, Grieve 2007), also taking into account newer considerations (Osinski *et al*. 2022).

The Mizarai crater revealed the allochthonous (allogenic) lithic impact breccia, allochthonous impact melt-bearing breccia (suevite), impact melt rocks, and presumably, also paraautochthonouslithic impact breccia (Fig. 5). The ejecta, forming the rim, or distal layers were not fixed in the boreholes surrounding the crater.

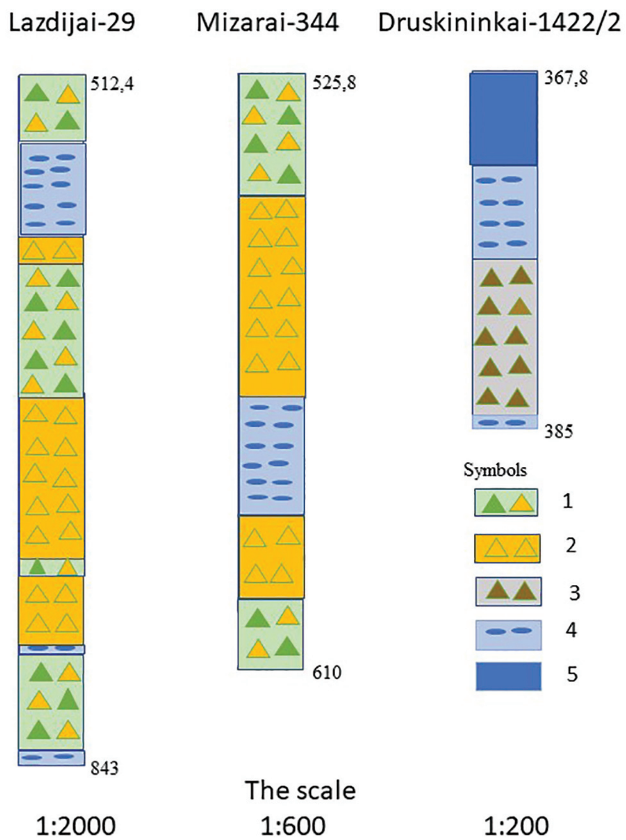

Fig. 5 Generalized sections of boreholes drilled in the Mizarai crater. Symbols: 1 – allochthonous lithic impact breccia; 2 – same, composed predominantly of granite fragments; 3 – same, composed predominantly of granodiorite and tonalite fragments; 4 – suevite; 5 – impact melt rock; the numbers – depth in meters

Allochthonous lithic impact breccias

The drill core from the allochthonous (allogenic) breccia was acquired by three boreholes drilled inside the crater – Lzd-29, M-344, and D-1422 (Table 1; Fig. 5). Rocks of this type are predominant in the crater. The breccia is composed mainly of fragments of rocks of various types, forming intervals of up to 49 meters. It consists of fragments of the igneous and metamorphic rocks of the crystalline basement whose size varies from tiny up to a few tens of meters and a matrix composed of the same material but finer-grained. Secondary minerals, mainly hydrothermal alteration products (carbonates, chlorite), and others are often present.

The rocks in fragments are divided into three groups according to their origin and presumable age:

- supracrustal (metasedimentary and metavolcanic) rocks;
- intrusive rocks ranging from gabbro to tonalite, presumably phases of the Randamonys suite;
- granitic rocks presumably of Mazovian–Veisiejai or Kabeliai suites.

Supracrustal rocks are represented by biotite-quartz-plagioclase gneisses, often with hornblende and K-feldspar. Gneisses are fine (< 1 mm) and evenly grained. In some fragments, there appear the signs of porphyritic texture formed by elongated (up to 3 mm) plagioclase crystals in the fine-grained matrix. The phenocrysts are euhedral or hypidiomorphic, some with simple twins. The protolith rocks of felsic gneisses are andesitic and dacitic metavolcanics (Fig. 6A, B).

Other members of the supracrustal group are amphibolites, after basalt and diabase, fine-grained, gneissic, often with relic diabase texture, in places with phenocrysts of plagioclase up to 3 mm long, euhedral, some crystals with zonality (Fig. 6C).

Originally intrusive rocks, in fragments, are gabbro, gabbro-diabase, diorite, quartz diorite, and tonalite characteristic of Randamonys intrusion and its satellite bodies (Fig. 7A). The rocks are affected by regional metamorphism of amphibolite facies, migmatized, and some are gneissic. The most abundant are fragments of granite, containing biotite, rarely hornblende, muscovite, and garnet (bh. Lzd-29/744 m; Lzd-29/765.5 m). The rocks are medium- to coarse-grained (5–10 mm), massive. They are comparable with Kabeliai or Mazury–Veisiejai granitic suites, whose age is 1.53–1.48 Ga. The bodies of these rocks, except garnet-bearing granite, are fixed also outside the crater (Fig. 7B).

The monomictic allochthonous breccia is mostly after granite. The granite appears in the form of fragments of various sizes, up to tens of meters thick blocks, deformed in particular bands mainly along the contacts (Fig. 5). The breccia is cemented by fine clasts of the same material and products of their chemical alteration (pelitic material, carbonates, iron oxides, chlorite).

Suevite

Suevite is fixed in the boreholes M-344, int. 576–590.2 m; Lzd-29, int. 530.6–575.3, 787–787.7, and 837.1–843 m; and D-1422, int. 372–377 and 384.7–385 m (Fig. 8). It is not always possible to recognize

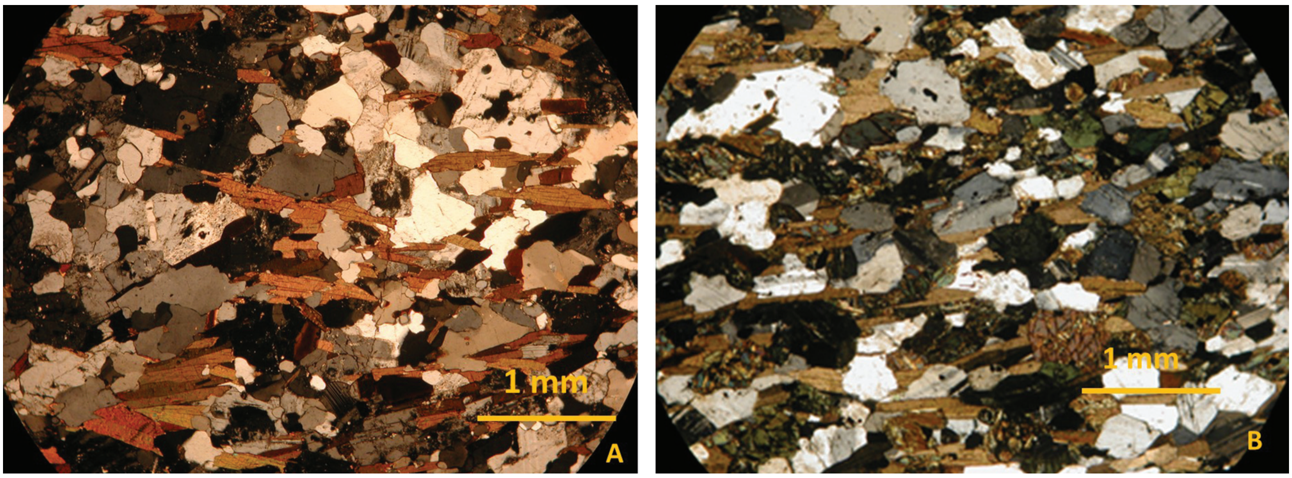

Fig. 6 Micrographs of supracrustal metamorphic rocks in the allochthonous breccia of the Mizarai crater: A – biotite-quartz-plagioclase gneiss, borehole Lzd-29/746.5 m; B – amphibolite, borehole Lzd-29/542.2 m; crossed polars

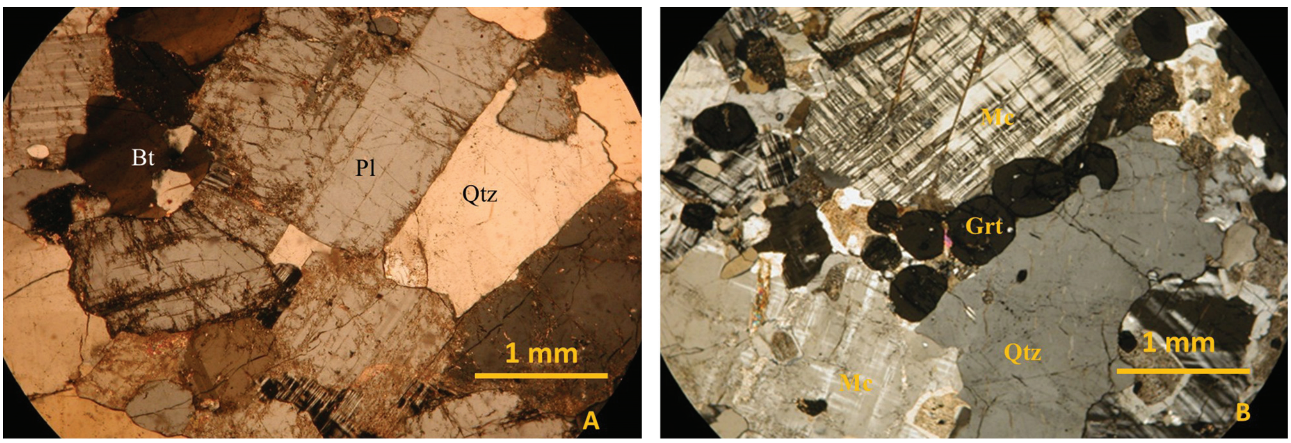

Fig. 7 Micrographs of intrusive rocks in the allochthonous breccia of the Mizarai crater: A – tonalite, borehole Lzd-29 /583.4 m, B – garnetiferous granite, borehole Lzd-29/744–765.5 m; crossed polars. Abbreviations of minerals: Bt – biotite, Grt – garnet, Mc – microcline, Pl – plagioclase, Qtz – quartz

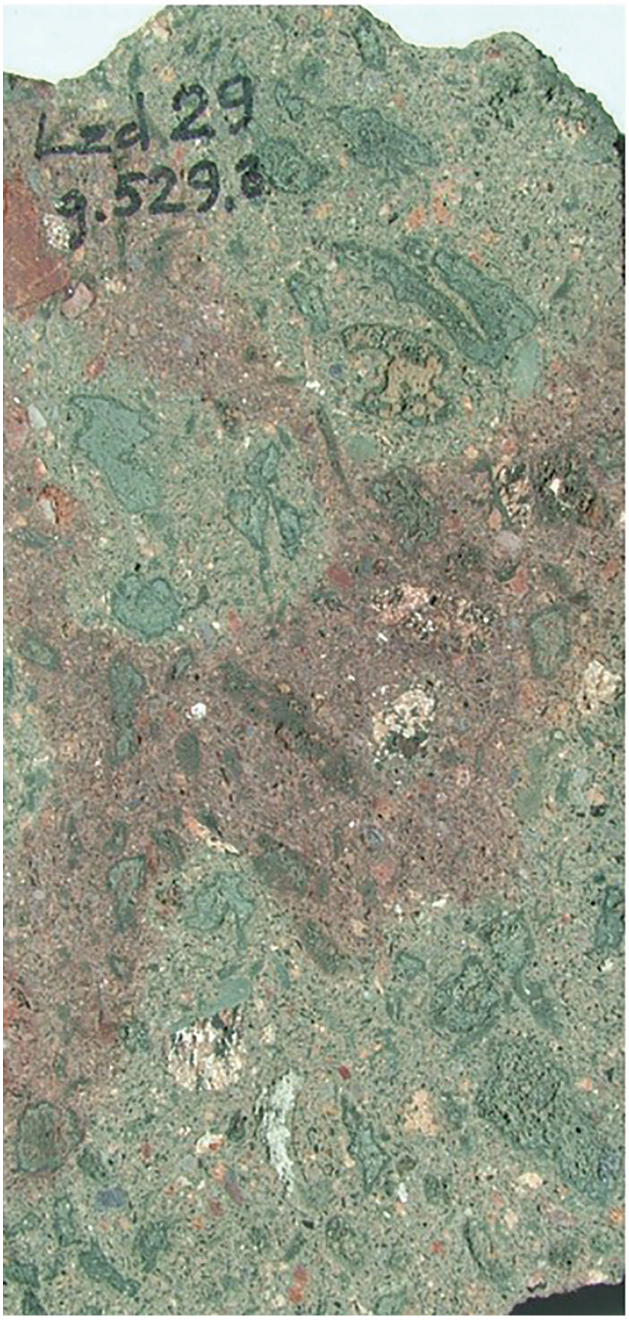

Fig. 8 Drill core of suevite: green inclusions – altered (chloritised?) glassy material; borehole Lzd-29/529.3 m; the diameter of drill core – 5 cm

glassy material in breccia in hand specimens; therefore, in fact the suevite might be more abundant. The fragments of target rocks in suevite are often subject to ductile deformation, have extended, wavy shapes, and probably were molten at various degrees. The glass inclusions are green or brown of irregular shape, of centimetres in size (Fig. 8). There are abundant smaller millimetre size fragments or shards of glass, some with fluidal structure, often containing crystallites and spectacular spherulites whose diameter is up to 0.1–0.14 mm (Fig. 9).

Impact glass

A 4.2 meters thick interval of glass was drilled by the borehole D-1422, interval 367.80–372.0 m. It appears on the contact of the allochthonous breccia and brecciated granodiorite, which presumably represents an autochthonous breccia.

In the boreholes D-1422, depth 358 m, and D-270, depth 358.5 m, the fragments of glass of centimetre size were found in the sandstone of the crater fill (Fig. 10A).

The groundmass of glass is amorphous but contains crystallites and ~ 0.01 mm long needle-shape crystals, presumably of plagioclase.

The impact melt usually appears in craters where the target is igneous and metamorphic rocks and the diameter is at least 5 km (Dressler, Reimold 2001). Thus, the appearance of glassy rocks in the Mizarai structure is in concert with its presumed size and target lithology.

Autochthonous (?) breccia

Presumably autochthonous breccia was reached by the borehole D-1422. The section of the crater rocks, below the crater-fill sediments, started with a layer of impact glass (Fig. 5). Below in the interval of 372–377 m, there appears monomict breccia, consisting of angular fragments of granodiorite of a millimetre to decimetre size. Deeper, up to the end of the borehole (depth 377–385 m), the same granodiorite was observed; it was fractured, but the fractures were predominantly closed. Breccia appears in bands up to 10 cm wide. Granodiorite is cut by centimetre size veins of the impact melt rock, with sharp contacts (Fig. 10B). In drill cores, we can see the fragments of rocks and crystals in groundmass of the impact melt rock, which appear isotropic under the microscope (Fig. 11). However, a more detailed investigation of these rocks by microprobe technique under SEM was not undertaken.

The monomict composition of breccia, its position below the impact glass body and injection veins implies the classification of this breccia as autochthonous, reached by erosion in the marginal part of the crater. In this marginal part of the crater, seismic exploration was not carried out, while on the seismic section (Fig. 3) the contact between these two types of breccia is not manifested as a reflector.

GEOCHEMICAL CHARACTERISTICS

The composition of the fragments of target rocks and suevite have been characterized by analyses for major oxides, produced by the conventional "wet chemistry" technique by two samples taken from the

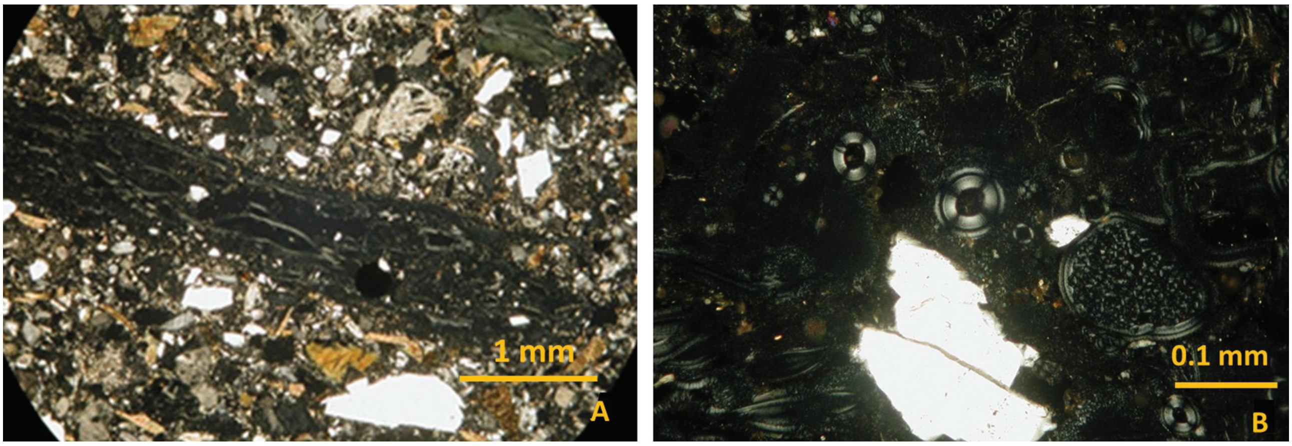

Fig. 9 Micrographs of glass fragments in suevite: A, B – borehole Lzd-29/547.6 m; crossed polars

Fig. 10 Impact melt rocks: A – fragments of the impact melt rock in the sandstone of the sedimentary fill of the crater, size – 3 × 4 centimetres; borehole D-1422/352.5 m; B – granodiorite, with veins of impact glass; borehole D-1422/373.2 m; the diameter of drill core – 5 cm

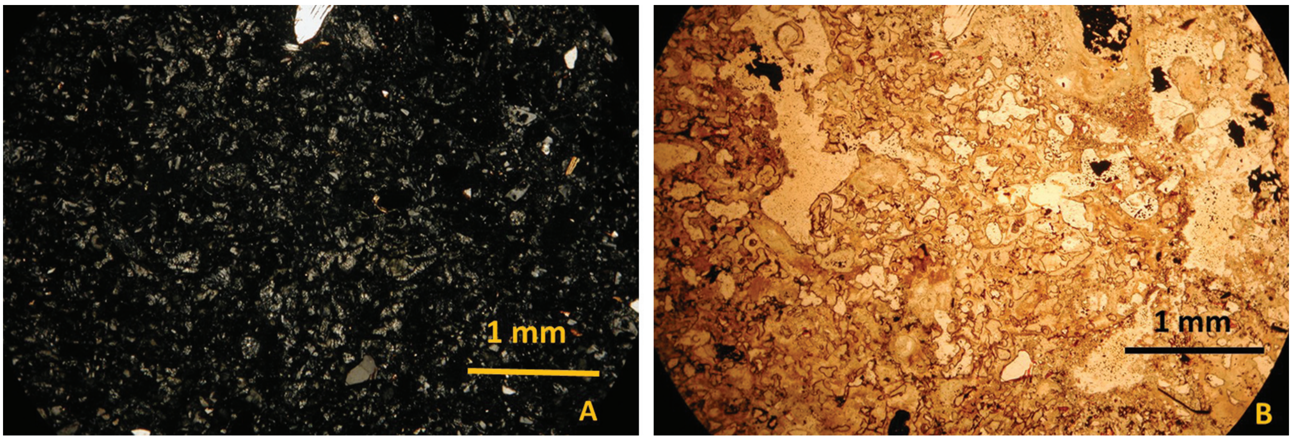

Fig. 11 Micrograph of glass in veins, borehole D-1422/378.6 m; A – crossed polars; B – parallel polars

glass body met in borehole D-1422, depth 368 and 373 m, and two samples of glass fragments from the crater-fill (boreholes D-1422, depth 356 m, and D-270, depth 358.8 m). Both fragments are from the lower part of the crater-fill sedimentary sequence and plausibly are the products of erosion of the impact glass bodies, which were and may remain in the vicinity. Also, the fragments of metagabbro-diabase from the breccia in borehole M-344/531.5 m were sampled (Table 3).

On the "Total Alkali *vs*. Silica" diagram (Fig. 12), the majority of analyses form clusters corresponding to the main lithologies found in the fragments of breccia. The fragments of metagabbro and amphibolite (whose protolith is mainly basalt or diabase) plot in the field of basalt. Part of amphibolite symbols are hidden by gabbro symbols. Two analyses appear in the field of ultrabasic and alkaline rocks, presumably because of hydrothermal alteration. The biotite-quartz-plagioclase gneisses, presumably felsic metavolcanics, plot in the field of and andesite. Suevite analyses form clusters in the field of the intermediate rocks of the sub-alkaline series.

The composition of glass fragments in the sedimentary fill is close to the composition of gabbro. The composition of two samples taken from the body of impact glass in borehole D-1422, (depth 368 and 373 m) is similar and corresponds to trachyandesite. A remarkable feature of glass is elevated alkalinity expressed in the content of potassium. In the glass from the sheet cut by the borehole D-1422, the content of potassium is particularly high (K_2O = 11.4%), while the content of sodium and calcium is around 1%. A higher alkalinity of suevite might be due to the admixture of impact glass, the alkalinity of which in all analyzed samples is elevated due to a higher amount of potassium.

The elevated content of potassium in the impact glass was reported also in some other impact craters: Brent (Canada) – 5.07%, Haughton (Canada) – 11.59%, Ilyinets (Ukraine) – 9% (Dressler, Reimold 2001), Logoisk (Belarus) (Glazovskaja *et al*. 1991). In Gow Lake crater (Canada) impact melt bearing rocks K_2O content exceeds 10%, while in same rocks Na_2O is up to 1%, and CaO up to 0.8% (Osinski et al. 2023). This phenomenon is explained by a different mobility of sodium, calcium and silica as compared to potassium in the course of vaporisation of rocks (Parfionova, Yakovlev 1977; 1982) or selective melting of K-feldspar and enrichment of melt by potassium (Glazovskaja *et al*. 1991; Osinski *et al*. 2022).

The composition of two fragments of glass taken from the sedimentary cover are different and reveal affinity to basic and ultrabasic rock.

Table 3. Composition of glass from the Mizarai crater

Sample	SiO_2 %	Al_2O_3 %	Fe_2O_3 %	MgO %	CaO %	Na_2O %	K_2O %	TiO_2 %	P_2O_5 %	MnO %	Cr_2O_3 %	Ni ppm	Sc ppm
270/358.5	46.63	19.90	7.70	5.97	0.95	0.82	4.45	0.88	0.03	0.07	0.010	46	23
344/531.5	49.47	16.11	9.82	9.86	2.03	2.42	1.13	1.12	0.24	0.09	0.019	122	21
1422/356	40.27	13.52	18.42	12.27	0.46	0.98	2.35	0.60	0.03	0.09	0.010	105	25
1422/373	56.5	16.9	6.46	3.83	0.94	0.72	11.3	0.51	0.14	0.06	N.A.	39.2	9.3
1422/368	55.89	16.29	5.64	3.88	1.13	0.79	11.49	0.54	0.12	0.05	0.011	41	12

Sample	LOI %	Ba ppm	Co ppm	Cs ppm	Ga ppm	Hf ppm	Nb ppm	Rb ppm	Sr ppm	Ta ppm	Th ppm	Ni ppm	Sc ppm
270/358.5	12.3	753	12.5	3.5	25.4	5.2	8.9	64.0	160.6	0.7	13.5	5.3	150
344/531.5	7.4	296	35.7	1.5	20.2	3.4	6.7	35.5	223.7	0.4	3.5	1.2	170
1422/356	10.6	256	56.0	1.1	35.0	4.2	6.4	63.3	96.6	0.4	15.0	6.5	229
1422/373	3	641	15	N.A.	20.6	3.7	5.1	95	60	0.42	8.8	3.32	75
1422/368		595	16.5	0.1	20.6	3.5	6.3	100.5	73.6	0.5	10.5	2.7	79

Sample	W ppm	Zr ppm	Y ppm	La ppm	Ce ppm	Pr ppm	Nd ppm	Sm ppm	Eu ppm	Gd ppm	Tb ppm	Ni ppm	Sc ppm
270/358.5	0.8	204.9	15.8	67.7	138.0	17.52	59.8	7.84	1.74	4.42	0.51	2.65	0.46
344/531.5	<0.5	137.4	13.0	27.5	57.3	6.87	25.4	4.38	1.08	3.47	0.51	2.97	0.48
1422/356	0.6	144.2	12.0	53.2	63.4	5.64	15.8	2.87	0.69	2.50	0.43	2.57	0.43
1422/373		144	17.8	N.A.	N.A.	N.A.	N.A.	N.A.	N.A.	N.A.	N.A.	N.A.	N.A.
1422/368	< 1	94.4	22.3	42	81.5	9.57	37	6.2	1.34	4.61	0.62	3.45	0.71

Sample	Er ppm	Tm ppm	Yb ppm	Lu ppm	TOT/C %	TOT/S %	Mo ppm	Cu ppm	Pb ppm	Zn ppm
270/358.5	1.47	0.25	1.66	0.25	0.15	0.03	0.2	288.9	7.3	67
344/531.5	1.42	0.21	1.33	0.19	0.06	<0.02	0.3	73.4	2.7	103
1422/356	1.17	0.18	1.06	0.15	0.07	<0.02	0.5	480.0	39.5	146
1422/373	N.A.	N.A.	N.A.	N.A.	N.A.	N.A.	1.05	150	N.A.	144
1422/368	2.14	0.29	1.91	0.29	N.A.	N.A.	< 1	143	10	95

The chondrite normalized REE abundance diagram demonstrates a tide cluster of lines. The REE are differentiated and enriched in LREE (Fig. 13).
The content of elements indicative of the sideritic impactor body (Ni, Co) is low, and even the highest values of Ni (up to 130 ppm) and Co (up to 56 ppm) (Fig. 14) do not exceed concentrations fixed in the rocks of Randamonys suite and supracrustal amphibolites outside the crater (Motuza 2022). They cannot be regarded as indices of contamination by impactor material but deserve attention for further investigations.

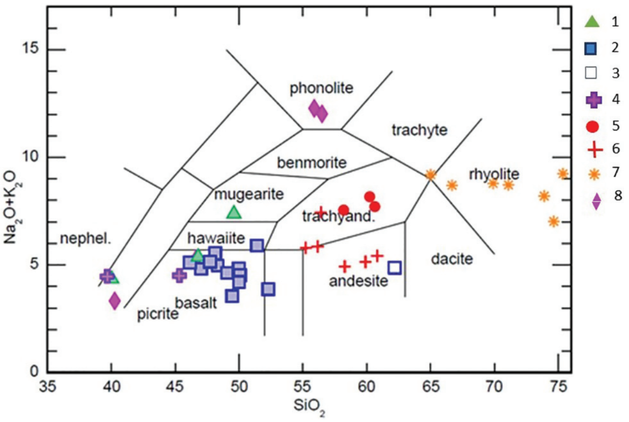

Fig. 12 Total Alkali *vs*. Silica diagram (after Cox *et al.* 1979) for the impact rocks from the Mizarai crater. Symbols: 1 – amphibolite; 2 – metagabbro; 3 – diorite; 4 – not identified hydrothermally altered rocks; 5 – suevite; 6 – supracrustal gneiss; 7 – granite; 8 – impact glass

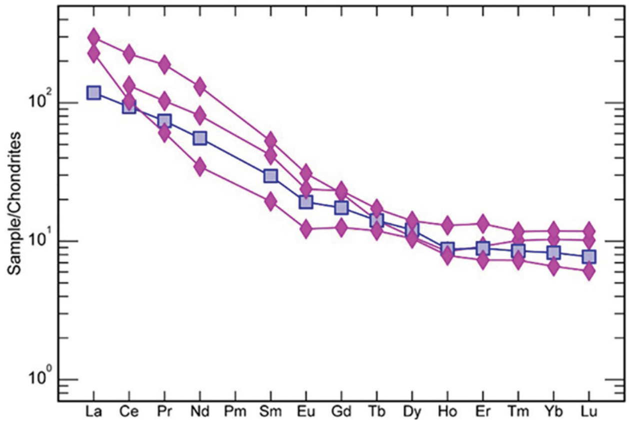

Fig. 13 Chondrite normalised REE abundance diagram for impact glass from the Mizarai crater. Symbols as in Fig. 12

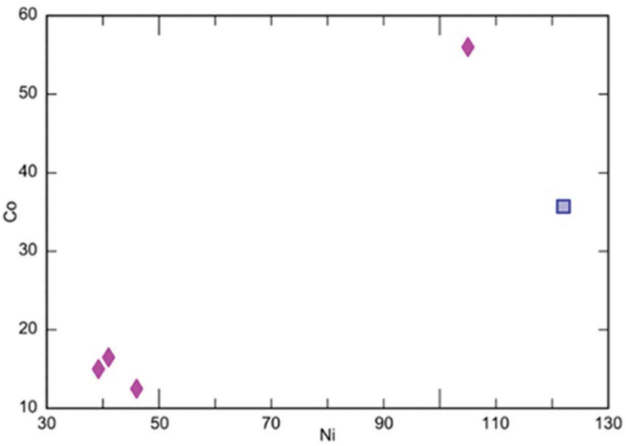

Fig. 14 Concentration of Co and Ni in impact glass from the Mizarai crater. Symbols as in Fig. 12

Two samples taken from non-identified, mainly biotitic or hydrobiotitic rocks, probably are the products of hydrothermal alteration, whose peculiarity is elevated alkalinity.

INDICATIONS OF THE HYPERVELOCITY IMPACT

In the Mizarai impact structure, the following principal indications of impact origin have been discovered: the shatter cones, Planar Deformation Features (PDFs), isotropization of quartz and feldspars, and kink-bands in biotite (Fig. 15).
Shatter cones are produced at comparative low pressure, 2–10 Pa. They appear both in simple and complex craters of various size, predominantly on central uplift, but also near rims, in main types of stratigraphic settings and all types of impactites. The formation of shatter cones remains enigmatic (Osinski *et al.* 2016), in spite of it they are regarded as unambiguous indications of shock metamorphism (Osinski *et al.* 2023).
The probability of finding shatter cones in the cores of eroded and buried simple craters is very low (Osinski *et al*. 2022). Nevertheless, in the Mizarai crater, shatter cones have been noticed in two out of four boreholes – M-344, drilled in the center of the crater, and D-1422 located in its marginal part. In the borehole M-344 (depth 534.5–536.2 m) a part of shatter cone was observed in a granite fragment in the polymictic breccia. It is in the form of the slightly undulating surface of fracture, with parallel striation (Fig. 15A).
In the borehole D-1422 (depth 377.4 m), spectacular shatter cones are observed in the brecciated granodiorite (Fig.15B), in form of striated, conical fractures of different strike and dip positions.
The PDFs of at least three directions are observed in quartz and microcline grains, and, less certainly, also in plagioclase. These structures appear under the 10 to 30 GPa in very variable setting, in most types of rocks from all boreholes, both in the upper part of the drilled section and in its bottom. In the borehole M-344, they are present in granite fragments from monomictic and polymictic breccia (Figs 15C; 16). The crystallographic orientations of PDFs in quartz from this rock was measured by R. Gailius (Motuza, Gailius 1980) applying conventional Universal Stage analysis. In a few quartz grains, he measured the angle between the quartz c-axes and the normal to the set of parallel fracture systems. The predominant angle is 21-24^{o} (Fig. 16), which is characteristic of shocked quartz.

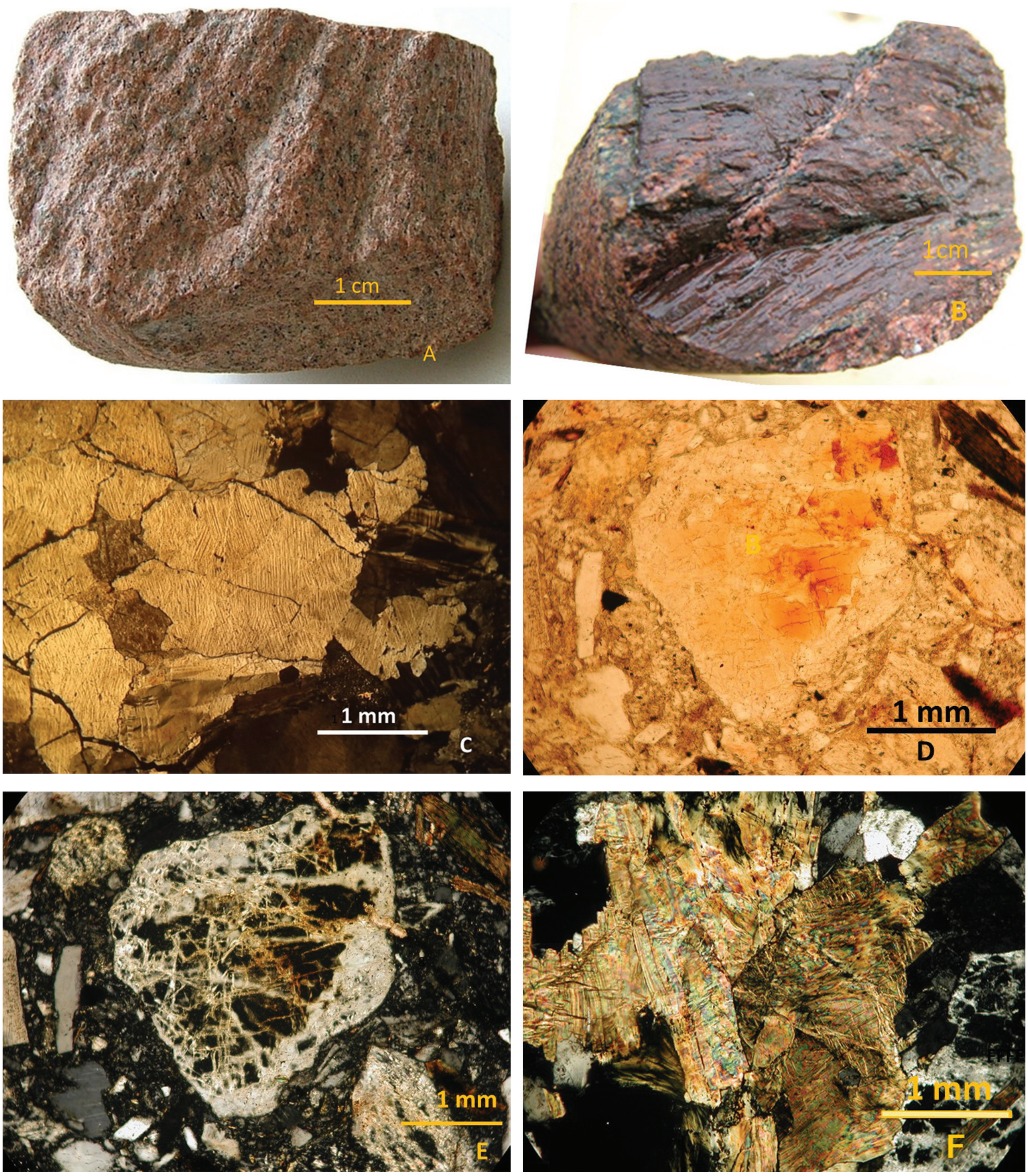

Fig. 15 Indications of the shock metamorphism in the impact rocks of the Mizarai crater. Shatter cones: A – borehole M-344/534.5-536.2; B – borehole D-1422/377.4 m; C – PDFs in quartz (borehole Lzd-29/559.2); D – isotropization of the plagioclase, parallel polars; E – same, crossed polars (borehole D-1422/376.8 m); F – kink-bands in biotite (borehole Lzd-29/559.2 m)

The solid state transformation of plagioclase, with the formation of maskelynite, and diaplectic glass after quartz, and kink-bands in biotite noticed in drill cores of all boreholes drilled inside the crater (Fig. 15D, E, F). The presented indications of the hypervelocity impact shall not be considered as strictly diagnostic. However, the set of indications presented, including shatter cones, makes the cosmic origin of the structure the most plausible option.

CONCLUSIONS

The estimated structural, petrological, mineralogical and geochemical features of the Mizarai structure and rocks in it provide a strong background to regard it as a hypervelocity impact crater.

The indications interpreted as shock metamorphism are: breccia, particularly suevite, impact melt rocks, PDFs forming a characteristic angle of c-axes

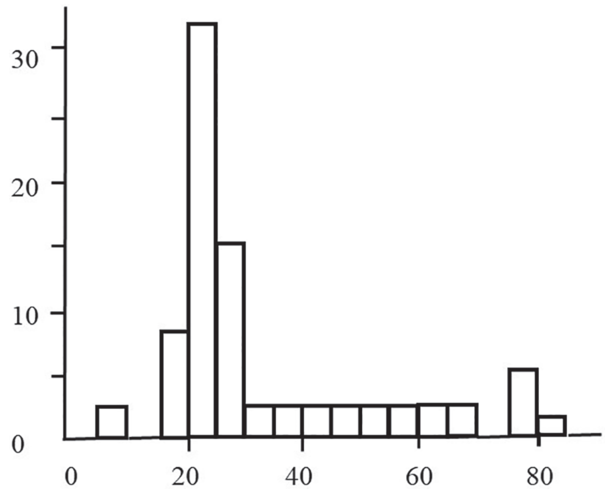

Fig. 16 Histogram of the distribution of the angle of c-axes in quartz and the normal to the PDFs in shocked rocks of Mizarai crater

in quartz, isotropization of quartz and feldspar, shatter cones noticed in the cores of two boreholes, and kink-bands in biotite.

The recent rim-to-rim size of the crater is 3.8 to 4.2 km. The rim-to-rim size of the primary crater, taking into account erosion in the course of 300 Ma, might be up to 5 km, and the depth slightly exceeded 1 km. No central uplift in the depression was revealed either by gravity or by seismic data, which requires it to be classified as a simple crater, though it is not typical for impact structures of such size.

The crater is filled up with presumably Ediacaran-Lower Cambrian sediments, whose maximal fixed thickness is 153.2 m. Their age is still the only argument for the estimation of the upper limit of the time of the impact.

In general, the geochemical patterns of impact rocks correspond to the composition of the target rock, while glassy rocks (impact melt rocks and suevite) demonstrate the elevated alkalinity caused by a high amount of potassium.

Some scholars refuse the cosmogenic origin of the Mizarai structure and presume its formation by volcanism, gas release, or just call it an "anomalous structure". However, such views are not supported by certain arguments, and indications of shock metamorphism are not interpreted in a different way (Suveizdis 2003; Kepežinskas 2001; Čyžienė *et al*. 2007).

ACKNOWLEDGEMENTS

The authors are highly thankful to anonymous reviewers, whose great competence and efforts contributed essentially to the quality of this paper. We acknowledge the pioneering research of the Mizarai crater by late Dr. Rimantas Gailius.

REFERENCES

Apirubytė, R., Gedvilaitė, N. 1969. Some specific patterns of the gravitational and magnetic fields in the Southeastern part of Lithuania, for instance of the Druskininkai area. In: *Proceedings of the scientific conference of young scientists-geologists of Lithuania* [In Russian].

Baliukevičius, A., Grigienė, A. 2015. Lithuanian impact craters. *Lithuanian Geological Survey. Annual Report* 77–82.

Baltrūnas, V., Šliaupa, A. 1974. The reconstruction of interglacial paleogeomorphology in the Druskininkai area using the method of geological mapping. *Proceedings of the Lithuanian Geological Scientific Research Institute 27*, 61–74.

Bogdanova, S.V., Page, L.M., Skridlaite, G., Taran, L.N. 2001. Proterozoic Tectonothermal History in the Western part of the East European Craton: $^{40}Ar/^{39}Ar$ Geochronological Constraints. *Tectonophysics 339*, 39–6610.

Cox, K.G., Bell, J.D., Pankhurst, R.J. 1979. *The Interpretation of Igneous Rocks*. London: Allen and Unwin, 450 pp.

Čyžienė, J., Baliukevičius, A., Šliaupa, S., Lazauskienė, J. 2007. A set of structural maps for the reference strata of the pre-Quaternary successions of Lithuania at a scale of 1:200 000. *Geological Survey of Lithuania. Annual Report* 30–32.

Dobrokhotova, E.S. 1957. *Method by E.S. Feodorof in petrography*, 84 pp. [In Russian].

Dressler, B.O., Reimold, W.U. 2001. Terrestrial impact melt rocks and glasses. *Earth Sciences Reviews 56*, 205–284.

Fettes, D., Desmons, J. (Eds) 2007. Metamorphic Rocks: A Classification and Glossary of Terms. *Recommendations of the International Union of Geological Sciences. Subcommission on the Systematics of Metamorphic Rocks.* Cambridge University Press, 256 pp.

French, B.M. 1998. Traces of Catastrophe: A Handbook of Shock-Metamorphic Effects in Terrestrial Meteorite Impact Structures (PDF). *LPI Contribution* No. 954. Houston: Lunar and Planetary Institute, 120 pp.

Gailius, R., Motuza, G., Šliaupa, A. 1975. The Mizarai depression in the Druskininkai area. In: *The newest results of the geological research in Lithuanian SSR*, 10–12 [In Russian].

Glazovskaja, L.I., Gromov, J.I., Parfionova, O.V., Ilkevich, G.I. 1991. *Lahojsk astrobleme*, 141 pp.

Graniczny, M., Satkunas, J., Motuza, G., Kowalski, Z., Čyžienė, J. 2011. Ciekawostki geologiczne Druskiennik (Druskininkai). *Przegłęd Geologiczny 59*, 206–210.

Hall, A.M., Putkinen, N., Hietala, S., Lindsberg, E., Holma, M. 2021. Ultra-slow cratonic denudation in Finland since 1.5 Ga indicated by tiered unconformities and impact structures. *Precambrian Research 352*, 106000. https://doi.org/10.1016/j.precamres.2020.106000

Jankauskas, T.V. 1989. *Mikrofossilii dokembrija SSSR* [*Microfossils of the Precambrian of the USSR*], 191 pp. [In Russian].

Judson, S., Ritter, D.F. 1964. Rate of regional denudation in the United States. *Journal of Geophysical Research 69*, 3395–3401. https://doi.org/10.1029/JZ069i016p03395

Kenkmann, T. 2021. The terrestrial impact crater record: A statistical analysis of morphologies, structures, ages, lithologies and more. *Meteoritics & Planetary Sciences 56(5)*, 1024–1070. Doi: 10.1111/maps.13657

Kepežinskas, K. 2001. *Evolution of the Magmatic Rocks in the Southeastern Baltic Region*. Vilnius, 154 pp.

Koeberl, C. 2002. Mineralogical and geochemical aspects of impact craters. *Mineralogical Magazine 66(5)*, 745–768.

Korabliova, L., Šliaupa, S., Nasedkin, V. 2003. Modelling of different geological bodies using GM-SYS programme (potential fields). *Geological Survey of Lithuania: Annual Report 2002*, 49–52.

Masaitis, V.L. 1999. Impact structures of North-eastern Eurasia: The territories of Russia and adjacent countries. *Meteoritics & Planetary Science 34*, 691–711.

Masaitis, V.L., Mashchak, M.S., Selivanovskaja, T.V., Raichlin, A.I., Danilin, A.N. 1980. Mizarai astrobleme. In: Pogrebickij, J.G. (Ed.): *Geology of the astroblemes*, 114–130 [In Russian].

Motuza, G. 2022. *The Precambrian geology of Lithuania: An Integrated Study of the Platform Basement Structure and Evolution*. Springer, 209 pp.

Motuza, G., Gailius, R. 1980. Mizarai meteorite crater. *Proceedings of the High schools of Lithuanian SSR. Geology 1*, 78 – 88 [In Russian].

Motuza, G., Šliaupa, S., Timmerman, M.J. 2015. Geochemistry and $^{40}Ar/^{39}Ar$ age of Early Carboniferous doleritesills in the southern Baltic Sea. *Estonian Journal of Earth Sciences 64*, 3. doi:10.3176/earth2015

Motuza, G., Spiridonov, A., Zamžickas, R. 2016. Record of Precambrian to Cambrian life in the Mizarai impact crater lake. *From Star and Planet Formation to Early Life*. *Conference abstracts.* Vilnius.

Osinski, R.G., Grieve, R.A.F., Ferriere, L., Losiak, A., Pickersgill, A.E., Cavosie, A.J., Hibbard, S.M., Hill, P.J.A., Bermudez, J., Marion, C.L.K., Newman, J.D., Simpson, S.L. 2022. Impact Earth: A review of the terrestrial impact record. *Earth-Science Reviews 232*, 104112.

Osinski, G.R., Coulter, A.B., Flemming, R.L., Ozaruk, A., Pickersgill, A., Singleton, A.C. 2023. Revisiting the Gow Lake impact structure, Saskatchewan, Canada. *Meteoritics & Planetary Sciences 58(6)*, 775–788. https://doi.org/10.1111/maps.13986

Parfionova, O.V., Yakovlev, O.I. 1977. Some peculiarities of selective evaporation in target rock after meteoritic impact. In: *Impact and explosion cratering*. Pergamon Press. New York, 843–860 pp.

Parfionova, O.V., Yakovlev, O.I. 1982. Petrochemical peculiarities of impactite and importance of processes of vaporization and condensation in course of formation of impact craters. *Meteoritics 40*, 113–122.

Puura, V., Lindström, M., Floden, T., Pipping, F., Motuza, G., Lehtinen, M., Suuroja, K., Murnieks, A. 1994. Structure and stratigraphy of meteorite craters in Fennoscandia and the Baltic region: a first outlook. *Proceedings of Estonian Academy of Sciences, Geology 43(2),* 93–108.

Rondot, J. 1994. Recgnition of eroded astroblemes. *Earth Science Reviews 35*, 331–365.

Stöffler, D., Grieve, R.A.F. 2007. Impactites. In: Fettes, D., Desmons, J. (Eds) 2007. *Metamorphic Rocks: A Classification and Glossary of Terms, Recommendations of the International Union of Geological Sciences.* Cambridge University Press, 82–91, 111–25, and 126–242 pp.

Suveizdis, P. 2003. *Lietuvos tektoninė sandara* [*Tectonic structure of Lithuania*]. Vilnius [In Lithuanian].

Šliaupa, A.I., Stirpeika, A.D. 1973. Volcanogenic-sedimentary deposits in South-western Lithuania. *Proceedings of the III scientific conference of Lithuanian geologists,* 60–62 [In Russian].

Zamžickas, R. 2012. *Mizarų smūginio kraterio sandara* [The structure of the Mizarai impact crater]. In: *Bioateitis: gamtos ir gyvybės mokslų perspektyvos, jaunųjų mokslininkų konferencija.* Vilnius: Lietuvos mokslų akademija [In Lithuanian].